SEMI-ANNUAL REPORT

(for January - June 1996)

Contract Number NAS5-31363

OCEAN OBSERVATIONS WITH EOS/MODIS:

Algorithm Development and Post Launch Studies

Howard R. Gordon
University of Miami
Department of Physics
Coral Gables, FL 33124

(Submitted July 15, 1996)

Semi-Annual Report (1 January - 30 June 1996) NAS5–31363

Preamble

As in earlier reports, we will continue to break our effort into seven distinct units:

- Atmospheric Correction Algorithm Development
- Whitecap Correction Algorithm
- k-water Radiance Distribution
- Residual Instrument Polarization
- Direct Sun Glint Correction
- Pre-launch Atmospheric Correction Validation
- Detached Coccolith Algorithm and Post-launch Studies

This separation has been logical thus far; however, as launch of AM-1 approaches, it must be recognized that many of these activities will shift emphasis from algorithm development to validation. For example, the second, third, and sixth will become almost totally validation-focussed activities in the post-launch era, providing the core of our experimental validation effort. Work under the fist bullet will continue into the post-launch time frame, but will be driven in large part by algorithm deficiencies revealed as a result of validation activities.

We will continue to use the above format for CY96 and CY97.

Semi-Annual Report (1 January – 30 June 1996) NAS5–31363

Abstract

Several significant accomplishments were made during the present reporting period.

- We have completed our basic study of using the 1.38 μm MODIS band for removal of the effects of thin cirrus clouds and stratospheric aerosol. The results suggest that it should be possible to correct imagery for thin cirrus clouds with optical thicknesses as large as 0.5 to 1.0.

- We have acquired reflectance data for oceanic whitecaps during a cruise on the *RV Malcolm Baldrige in* the Gulf of Mexico. The reflectance spectrum of whitecaps was found to be similar to that for breaking waves in the surf zone measured by *Frouin, Schwindling and Deschamps* [1996].

- We installed a CIMEL sun photometer at Fort Jefferson on the Dry Tortugas off Key West in the Gulf of Mexico. The instrument has yielded a continuous stream of data since February. It shows that the aerosol optical thickness at 669 nm is often <0.1 in winter. This suggests that the Southern Gulf of Mexico will be an excellent winter site for vicarious calibration.

- We completed a study of the effect of vicarious calibration, i.e., the accuracy with which the radiance at the top of the atmosphere (TOA) can be predicted from measurement of the sky radiance at the bottom of the atmosphere (BOA). The results suggest that the neglect of polarization in the aerosol optical property inversion algorithm and in the prediction code for the TOA radiances is the largest error associated with the radiative transfer process. Overall, the study showed that the accuracy of the TOA radiance prediction is now limited by the radiometric calibration error in the sky radiometer.

- W.M. Balch participated in two cruises (March and June) in the Gulf of Maine, a region of known dense populations of coccolithophore blooms. Considerable coccolith light scattering data were obtained with a flow-through instrument, along with data relating to calcite concentration and the rate of calcite production.

1. Atmospheric Correction Algorithm Development.

a. Task Objectives:

During CY 1996 there are four objectives under this task:

(i) Complete development of an algorithm module for removing the effects of stratospheric aerosol and/or cirrus clouds from MODIS imagery over the oceans.

(ii) Conduct research on the effects of strongly absorbing aerosols, and their vertical structure, on the existing atmospheric correction algorithm. Use the results of this research to develop a strategy for their removal.

(iii) Develop a detailed model of the diffuse transmittance of the atmosphere and the manner in which it is influenced by the angular distribution of subsurface upwelling spectral radiance. Add a module for this to the atmospheric correction algorithm.

(iv) Investigate the effects of ignoring the polarization of the atmospheric light field on the performance of the proposed atmospheric correction algorithm.

b. Work Accomplished:

A comprehensive report on the present status of the MODIS atmospheric correction algorithm was prepared for the Aerosol Remet e Sensing and Atmospheric Correction Workshop (sponsored by NASA/EOS). This was submitted to the *Journal of Geophysical Research*. A revised version is included in this report as Appendix 1. Several references to this Appendix are made in this report.

(i) Considerable progress was made regarding the influence of stratospheric aerosols on atmospheric correction, and the possibility of using the 1380 nm MODIS band for removing their effects. A paper has been prepared and submitted to *Applied Optics*. The paper is included in this report as Appendix 2. In Appendix 2 it is demonstrated that it should possible to perform a correction for cirrus clouds having optical thicknesses approaching unity. More work is required, however, to implement the algorithm.

(ii) As demonstrated in Appendix 1, strongly absorbing aerosols present a serious problem for atmospheric correction. The nature of the problem is two fold: (1) in contrast to weakly-absorbing aerosols, when the aerosol is strongly absorbing its distribution in altitude becomes very important; and (2) the technique of distinguishing aerosol type through examination of the spectral variation of the radiance in the near infrared, used by the correction algorithm, cannot distinguish between weakly-absorbing and strongly-absorbing aerosols. During this reporting period, we have tried to quantify the effect of the vertical structure, and to find ways in which to distinguish weakly- and strongly- absorbing aerosols.

One revealing simulation study was a series of computations in which the strongly-absorbing aerosol (the *Shettle and Fenn* [1979] Urban aerosol model at relative humidity 80% – U80) was confined to thin layer near the surface, as assumed in the correction algorithm, and then to layers 1 km thick progressively moved higher and higher in the atmosphere. Figure 1–1 provides examples of the variation of the radiance at the top of the atmosphere for as a function of the altitude of the l-km thick layer. In the figure, θ_0 is the solar zenith angle, and the viewing is either at the center of the edge of the MODIS scan. Z_{tOP} is the height of the top of the l-km thick aerosol layer. When $Z_{toP} = 0$ the aerosol is confined to a thin layer at the surface. The decrease in the radiance at the top of the atmosphere as the altitude of the layer increases is remarkably large at 443 nm where the contribution from molecular scattering is large. No such decrease is seen when the aerosol is nonabsorbing.

The radiances used to generate Figure 1–1 were used as pseudo data and introduced into the correct ion algorithm. The correction algorithm employed a set of candidate aerosol models having strong absorption (U80 was not among the set), i.e., it was assumed that somehow the fact that the aerosol was strongly absorbing had already been determined. The resulting errors in the retrieved water-leaving reflect ante (as a function of the height of the aerosol layer for several MODIS bands and viewing-solar geometries are presented in Figure 1-2.

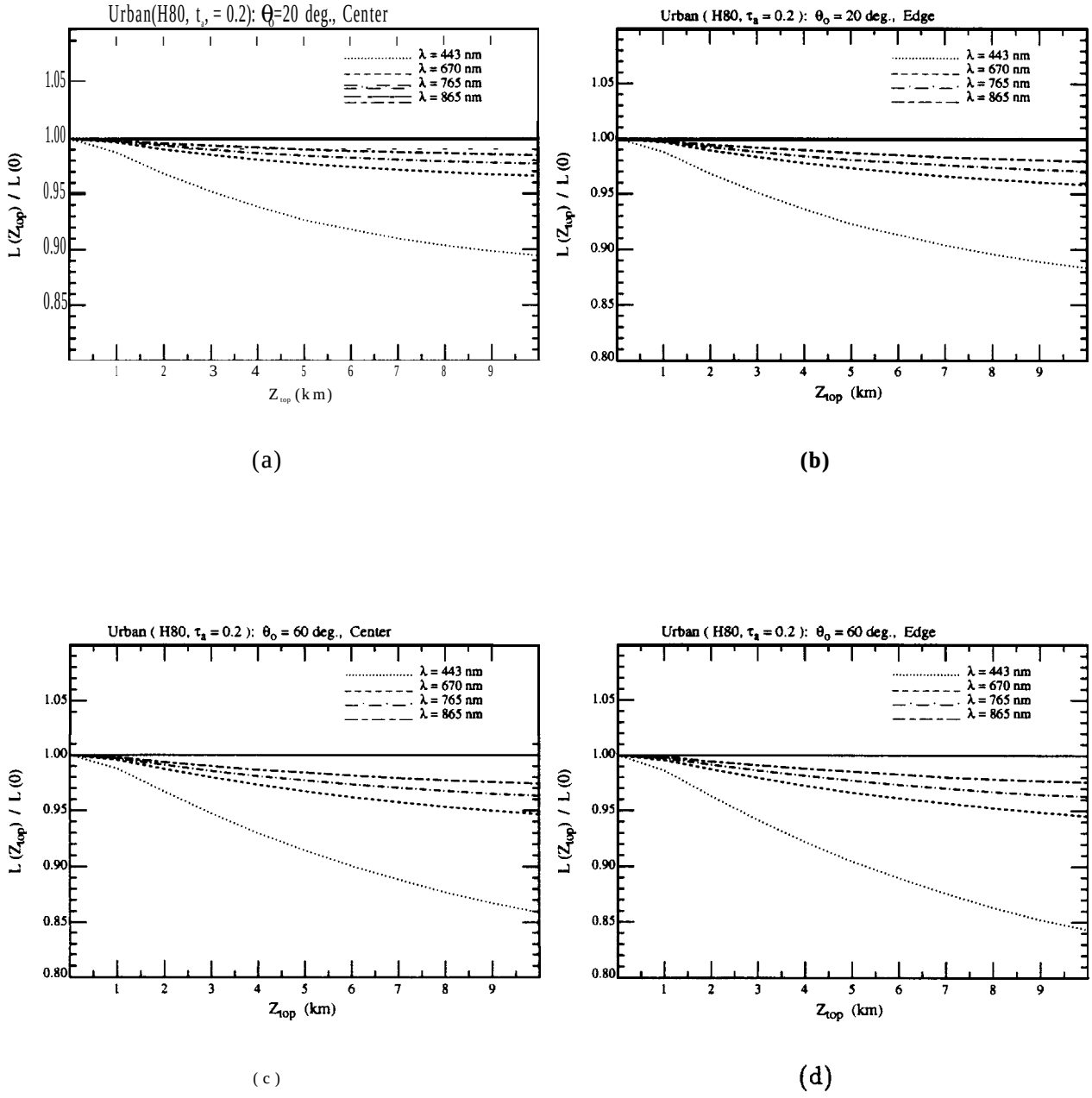

Figure **1-1.** Ratios of radiances for the U80 aerosol in a **1** km thick layer with the top at Z_{TOP}. (a) θ_0= 20°, viewing at center; (b) θ_0= 20°, viewing at edge; (c) θ_0= 60°, viewing at center; (d) θ_0= 60°, viewing at edge.

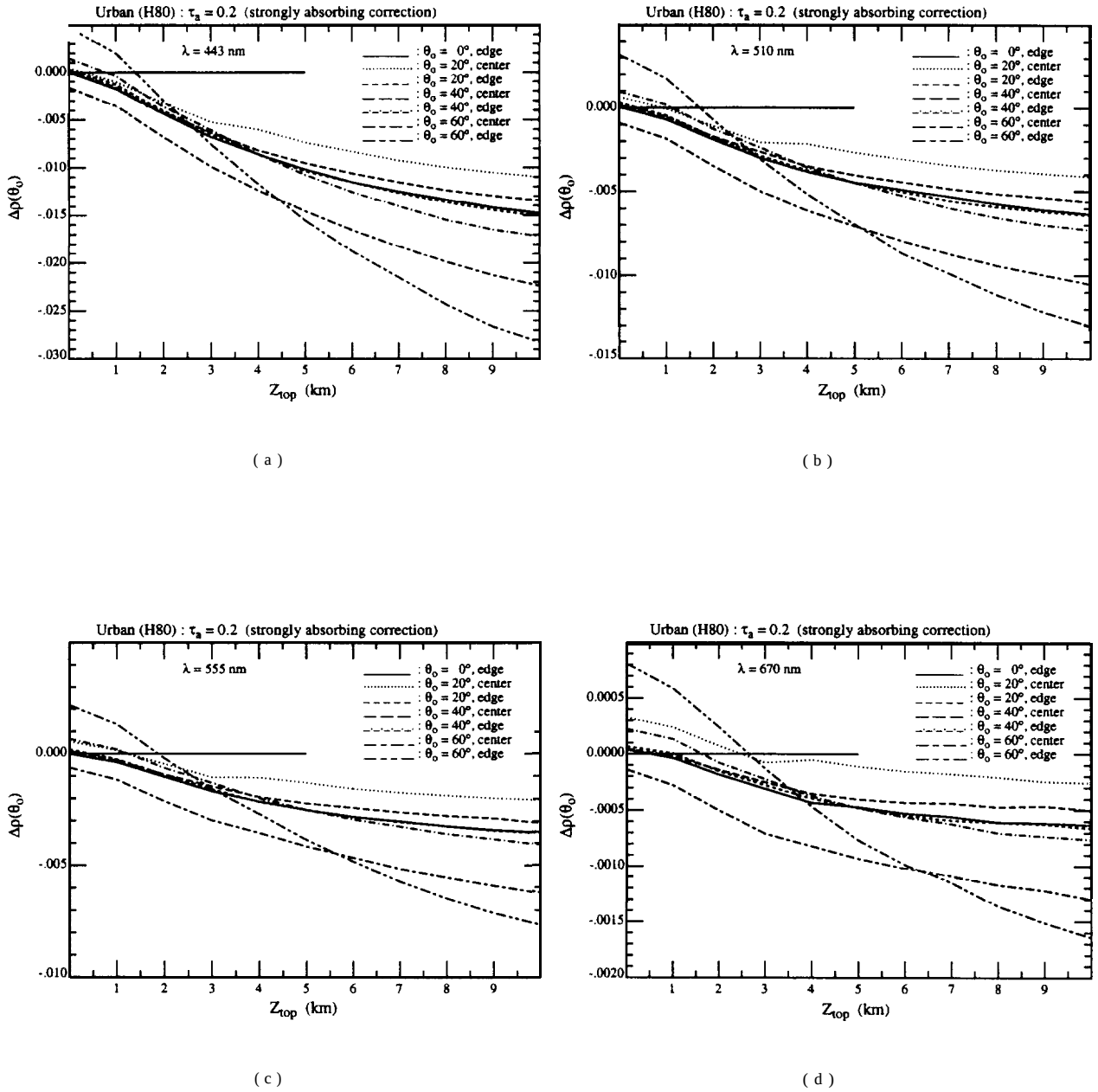

Figure 1-2. Vertical structure effects on the retrieval errors for U80 using strongly-absorbing aerosols as candidates: (a) λ = 443 nm, (b) λ = 510 nm, (c) λ = 555 nm, (d) λ = 670 nm.

The goal of atmospheric correction is $|\Delta\rho| < 0.002$ at 443 nm. If the aerosol is at the surface or uniformly distributed in a layer 1 km above the surface ($Z_{toP} = 1$), the algorithm meets the accuracy goal; however, if it is in a l-km thick layer the top of which is 2 km or higher above the surface ($Z_{tOP} \geq 2$ in Figure 1–2) the algorithm fails to meet the goal. This suggests that

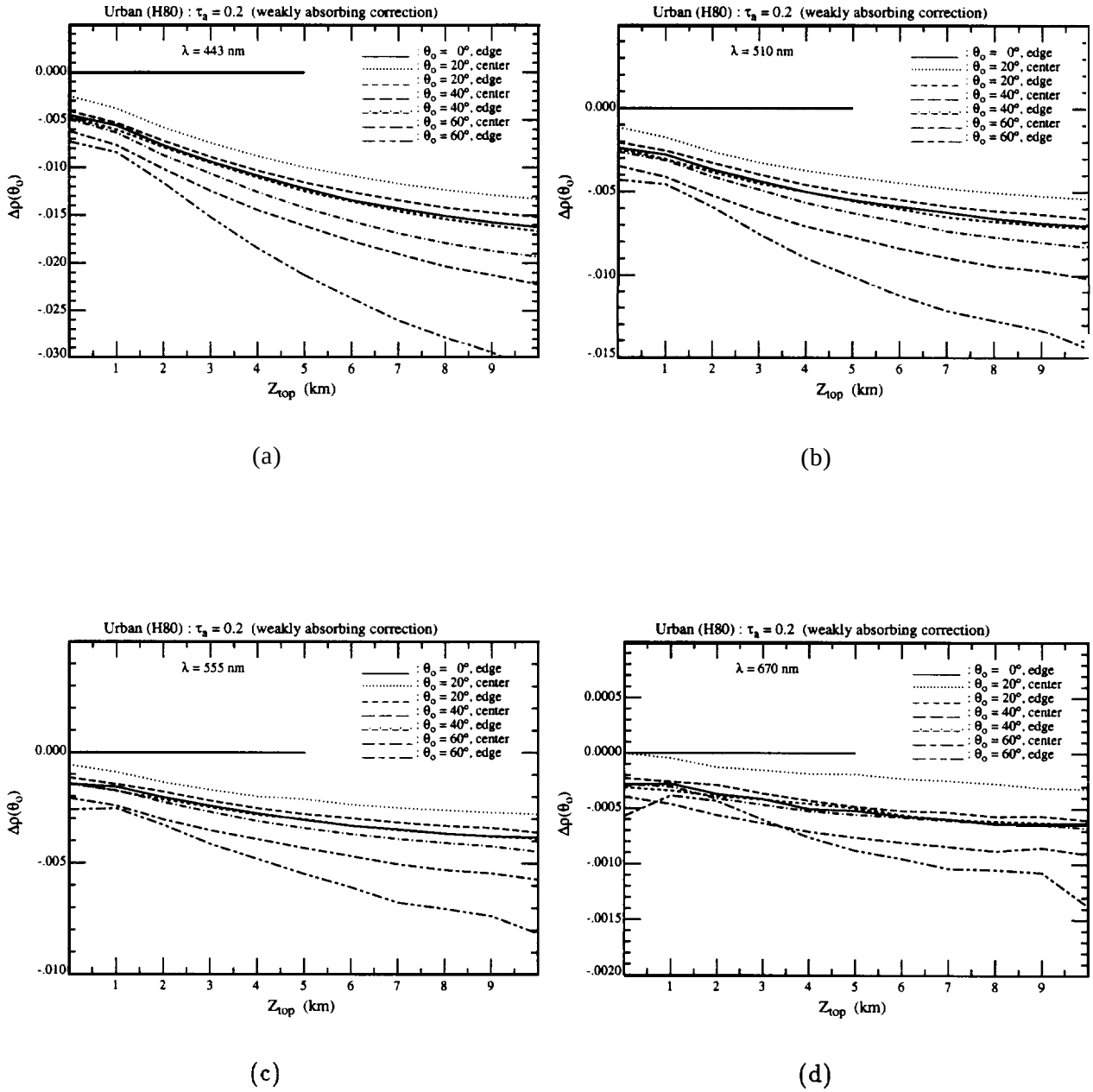

Figure 1–3. Vertical structure effects on the retrieval errors for U80 using weakly-absorbing aerosols as candidates: (a) λ = 443 nm, (b) λ = 510 nm, (c) λ = 555 nm, (d) λ = 670 nm.

the vertical placement of the absorbing aerosol must be known to within ±1 km. Earlier studies (Appendix 1), in which the same aerosol was uniformly mixed from the surface to an arbitrary altitude, also suggested that the thickness of the layer had to be known to within ±1 km. These results indicate that when strongly absorbing aerosols are present, e.g., urban pollution or desert

dust transported over the oceans, atmospheric correction will require that the candidates aerosol models also include candidate vertical distributions as well as aerosol types. This will considerably complicate the algorithm in such cases, and underscores the importance of a climatology of aerosol vertical distribution for oceanic regions influenced by strongly absorbing aerosols.

The result described above assumed that the presence of the strongly absorbing aerosol was not in doubt; however, at this time we have no method of detecting their presence. Figure 1–3 provides the results for the same simulations as in Figure 1-2 but with the normal (weakly-absorbing) aerosol models used as candidates, i.e., assuming that the presence of the strong absorption was not determined. Clearly, the results are poorer than those in Figure 1–2, possessing a negative-error bias. Thus, it is as necessary to know that the aerosol absorbs strongly as it is to know the vertical distribution.

We are examining several possibilities for detecting the presence of strongly-absorbing aerosols. One method we have tried for detecting the presence of strong absorption was examination of the atmospheric correction error at 670 nm. In this band, the water-leaving reflectance is generally low ~ 0.0005 to 0.001 in Case 1 waters (it was assumed to be zero in the CZCS atmospheric correction algorithm). The results in Figure 1–3 suggest that if the aerosol is strongly absorbing the water-leaving reflectance at 670 nm will have a negative bias of ~ 0.0005. Thus, if atmospheric correction yields a negative water-leaving radiance at 670 nm, it would be a sure indication of a correction problem. However, as the error is of the same order as the actual water-leaving reflectance at 670 nm, such a test will not always be valid, i.e., there will be false negatives, situations in which the aerosol strongly absorbs, but the retrieved water-leaving radiance at 670 will be positive.

Another possible way of attempting to detect absorbing aerosols, in particular desert dust, is to examine the behavior of the radiance reflected from the ocean-atmosphere system in the short - wave infrared (SWIR). In Appendix 1 (Section 4.2) it is suggested that the variation of the aerosol component of the reflectance from the NIR to the SWIR is significantly different for aerosols possessing refractive indices and size distributions representative of Saharan dust when compared

to nonabsorbing aerosols. This is shown in Figure 1–4 which provides the atmospheric correction ε parameter defined according to

$$\varepsilon(\lambda, 865) = \frac{\rho_{as}(\lambda)}{\rho_{as}(865)},$$

where $p_{as}(\lambda)$ is the aerosol contribution to the ocean-atmosphere reflect ante at a wavelength λ, for several aerosol size distributions. Note that the value of ε decreases more rapidly into the SWIR.

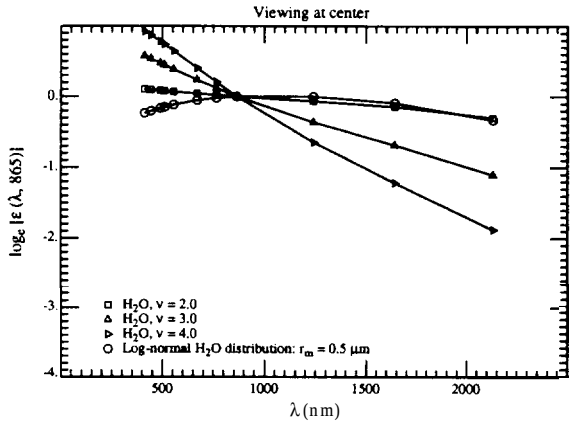

Figure 1-4a. ε(λ,865) for nadir viewing with θ_0= 60° for the Hase C models composed of liquid water.

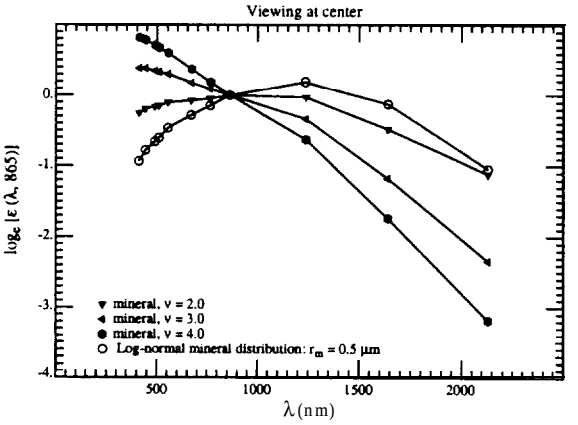

Figure l-4b. ε(λ,865) for nadir viewing with θ_0= 60° for the Haze C models composed of absorbing minerals.

for the Saharan dust compared with a similar sized aerosol possessing the refractive index of water. The source of this decrease appears to be a significant decrease in the real part of the refractive index of the dust. If this decrease is correct, the fact the dust particles are nonspherical would probably only minimally influence the sensitivity y of this method of detection.

Although such a method would likely be limited to Saharan dust (assuming the modeled index of refraction is correct) we have performed simulations aimed at determining whether the single scattering approximation could be used to implement a discrimination algorithm based on this idea in a simple manner. If we ignore multiple scattering in the aerosol contribution, then ε is approximateed by

$$\varepsilon_{\mathbf{Approx}}(\lambda, 865) = \frac{\rho_t(\lambda) - \rho_r(\lambda)}{\rho_t(865) - \rho_r(865)}, \quad (1)$$

where p_t is the total reflectance of the ocean-atmosphere system, and p_r is the contribution due to Rayleigh scattering. Figure 1–5 compares the value of $E_{Approx}(\lambda, 865)$ using this equation with the

true value for the Log-normal (largest T.(A) in the SWIR) model in Figure 1–4 and for aerosol optical thicknesses $\tau_a(865)$ of 0.3 and 0.4. Clearly, Eq. (1) provides an excellent approximation to $\varepsilon(\lambda, 865)$ in the NIR and SWIR for even large aerosol optical thicknesses. Thus, it appears that the SWIR could be used in a simple manner to distinguish Saharan dust from nonabsorbing maritime aerosols

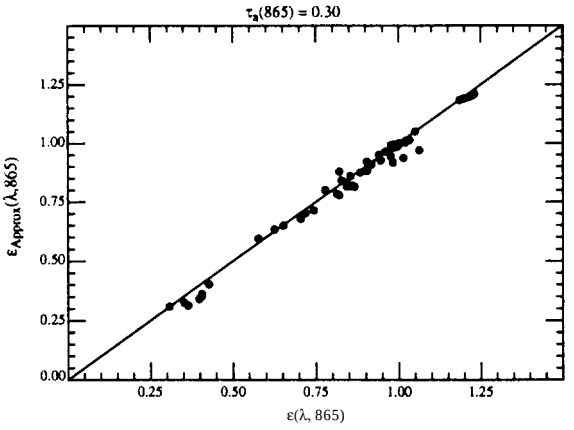

Figure 1–5a. Comparison between $\varepsilon(\lambda, 865)$ and $E_{Approx}(\lambda, 865)$ for several viewing geometries with $\tau_a = 0.30$.

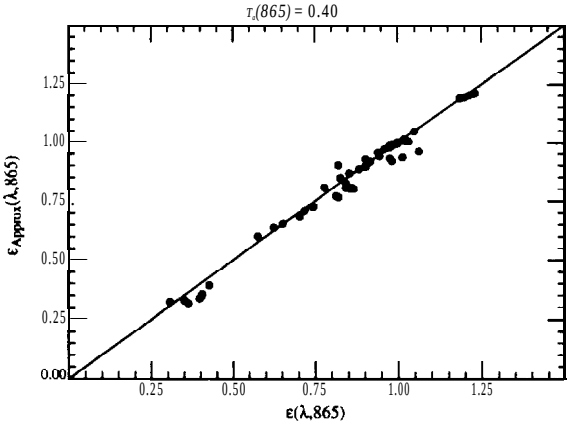

Figure 1–5a. Comparison between $\varepsilon(\lambda, 865)$ and $E_{Approx}(\lambda, 865)$ for several viewing geometries with $\tau_a = 0.40$.

by extrapolating and $E_{Approx}(865, 865)$ and $E_{Approx}(1260, 865)$ to find $E_{Extrapolated}(2130, 865)$. If $E_{Extrapolated}(2130, 865) \geq 2E_{Approx}(2l30, 865)$, it would indicate the presence of Saharan dust.

Finally, we are examining a new concept for distinguishing absorbing aerosols, in which a bio--optical radiate model, e.g., *Gordon et al.* [1988], is used to predict the water-leaving reflectance as a function of λ and pigment concentration (C). The value of *C* and the aerosol optical depth at 865 nm are then varied to provide $p_t(\lambda)$ for each aerosol model. The values of *C*, $\tau_a(865)$ and the aerosol model which yield the best fit (in an RMS sense) to the measured $p_t(\lambda)$ are taken to be correct. Initial tests suggest that this may work well for low C', e.g., $\leq$ 0.5 mg/m^3. The algorithm is very slow and probably could not be applied on a pixel-by-pixel basis; however, it may be possible to apply it on a regional basis.

(iii) The basic correction algorithm yields the product of the diffuse transmittance *t* and the water-leaving reflectance p_w. However, *t* depends on the angular distribution of p_w. If p_w were uniform, *t* would be easy to compute, and this approximation has always been employed in the past.

In **a** series of papers Morel and Gentili *[Morel and Gentili,* 1991; *Morel and Gentili,* 1993] studied theoretically the bidirectional effects as a function of the sun-viewing geometry and the pigment concentration. Their simulations suggest that, although the bidirectional effects nearly cancel in the estimation of the pigment concentration using radiance ratios, ρ_w can depend significantly on the solar and viewing angles. (Our major task number 3, a study of the in-water radiance distribution, experiment ally addresses this problem.)

In this reporting period, we initiated a study to understand the effect of bidirectional effects on the diffuse transmittance *t.* Through the use of the reciprocity y principle, we were able to develop a simplified method of computing *t,* given the upward radiance distribution with direction just beneath the sea surface. Although the study has only just begun, it appears that the difference between *t* (the correct diffuse transmittance) and *t** (the diffuse transmittance computed by assuming the subsurface upward radiance is uniform) is typically $\leq$ 4%, and is a relatively weak function oft he aerosol optical thickness. Thus, considering the error likely to result from the removal of the aerosol path radiance, it appears that in the blue ***t can*** be replaced by t^{-}, except in waters with low pigment concentrations, e.g., $\leq$ 0.5 mg/m^3.

(iv) We have performed no new numerical experiments concerning the effect of ignoring polarization in preparation of the aerosol reflect ante look up tables. Rather, we now include polarization in most of our simulations, e.g., those provided in Figures 1–1, 1–2, and 1–3. Our results thus implicitly contain the polarization effect. We do not plan any more polarization-specific studies.

c. Data/Analysis/Interpretation: See item b above.

d. Anticipated Future Actions:

(i) We must now develop a strategy for implementation of the cirrus cloud/stratospheric aerosol correction into the existing atmospheric correction algorithm. Specific issues include (1) the phase function to be used for the cirrus clouds, (2) the details of making two passes through the correction algorithm, (3) removal of the effect of water vapor above the clouds, and (4) preparation of the required tables. These will be addressed during the remainder of this calendar year with the goal

of answering all of the questions; however, actual preparation of the required look up tables will not begin until CY 1997.

(ii) We will continue the study with the goal of having a conceptual algorithm (or candidate algorithms) by the end of CY 1996. As our work has shown that a knowledge of the vertical distribution of the aerosol is critical, if it is strongly absorbing, we will begin procurement of a micro pulse lidar (MPL) system for use at sea on validation cruises, and from an island (likely Barbados) in the Saharan dust zone, to begin to compile a climatology of the vertical distribution required to adopt candidate distributions for use in this area.

(iii) We will develop a set of lookup tables for t^* to be used with the individual aerosol models. This will be coded and a module will be added to the correction algorithm utilizing these tables. We will attempt to devise a simple method of modifying t^* to form t at least for low pigment concentrations. This will require a model of the subsurface BRDF.

(iv) We will continue to use our vector radiative transfer code to generate pseudo test data; however, specific studies of the effect of polarization on atmospheric correction are being discontinued.

Additional task for CY96: We will initiate a study to determine the efficacy of the present atmospheric correction algorithm on removal of the aerosol effect from the measurement of the fluorescence line height (MOD 20).

e. Problems/Corrective Actions:

(i) None.

(ii) None.

(iii) None.

(iv) None.

(v) None.

f. Publications:

H.R. Gordon, Atmospheric Correction of Ocean Color Imagery in the Earth Observing System Era, Revised to *Journal of Geophysical Research, Atmospheres.*

H.R. Gordon, T. Zhang, F. He, and K. Ding, Effects of stratospheric aerosols and thin cirrus clouds on atmospheric correction of ocean color imagery: Simulations, Submitted to ***Applied Optics.***

2. Whitecap Correction Algorithm (with K.J. Voss).

a. Task Objectives:

As described in earlier reports, a whitecap radiometer system has been built and tested to provide a database for developing and validating the whitecap correction algorithm, as well as for providing an estimation of the whitecap contribution to the water-leaving radiance during the post-launch validation phase. The database includes spectral information as well as variables associated with the formation and occurrence of whitecaps such as wind speed and air/sea temperature.

b. Work Accomplished:

The software for data acquisition has been modified in order to increase observation time during whitecap events and GPS data, UTC time is updated less often (at 30 second intervals). The 6 channel upwelling radiometer, downwelling irradiance collector (deck cell) and air/water temperature, wind speed and direction are now acquired at ~ 7 samples per second. The video image from the TV camera mounted along side the radiometer to visually observe the water surface during data acquisition is also time/date stamped at the higher rate. This higher acquisition rate provides spectral information on a whitecap as it passes through its various stages of growth and decay. However, it should be noted that tracking a particular part of a whitecap is rare as the speed and direction in which the ship moves is rarely the same speed and direction in which a whitecap moves over the water surface.

From 29 March to 18 April 1996 the whitecap radiometer system was deployed on the NOAA ship *RV Malcolm Baldrige* on a cruise from Miami to a test location in the Gulf of Mexico, approximately 70 miles off shore from Cedar Key (Florida) in the Apalachicola Bay. The location provided relatively warm waters (16°-17°C) with a number of cold fronts moving off the mainland. These fronts usually lasted a couple of days bringing strong winds (sometimes as high as 18 m/s) and lowering the air temperature to about 120 C. The occurrence of an unstable atmosphere and good winds provided an interesting spectral whitewater data set.

Analysis software using Matlab has been developed to provide spectral reflectance values of different whitewater types, ranging from fresh thick foam as the waves begins to break to thin residual streaks and patches just before the whitewater is absorbed back into the ocean. In addition, software to estimate the effective augmented spectral reflectance of these different whitewater types and the total augmented spectral reflectance on the water leaving radiance for particular sea state conditions has been developed.

Although the effect of whitecaps on useful satellite data is generally restricted to their occurrence in cloud free regions and with data acquired around solar noon, whitecap events during this cruise were measured under a greater variety of sky conditions and times during the day to take full advantage of ship time. This combination of various solar zenith angles and overcast, diffuse to pat thy, and clear sky conditions, pushes the capability of the radiometer/deck cell relationship, established from laboratory calibration, in providing true reflectance measurements under all these conditions. Performance characterization of the radiometer and deck cell calibrations for conditions similar to that experienced dining the cruise is being quantified in terms of both the angular response of the calibration reflect ante plaque and the cosine collector of the deck cell under various lighting conditions.

c. Data/Analysis/Interpretation

An example of two whitecaps passing under the radiometer is shown in Figure 2-1. The 96 consecutive samples shown below are acquired over a period of ~ 15 seconds. In this example a large whitecap suddenly breaks in view of the radiometer with thick white foam (sample point 11) reaching a peak reflectance of ~ 55%. Six traces are plotted representing the six radiometer channels (410, 440, 510, 550, 670 and 860 nm). The lower trace corresponds to the 860 nm reflectance. The thick foam is temporarily replaced by a region of submerged bubbles and less thick foam (~ sample points 13, 14, 15) and some thick foam comes into view again at sample point 17. At sample point 20 and 21 a thin layer of foam passes followed by the decaying thicker foam to about sample point 35. Sample points from about 35 to 55 show the reflectance of thinning residual foam. Prom 60 to about 75 the reflectance of the foam free water surface is shown and is suddenly followed by another

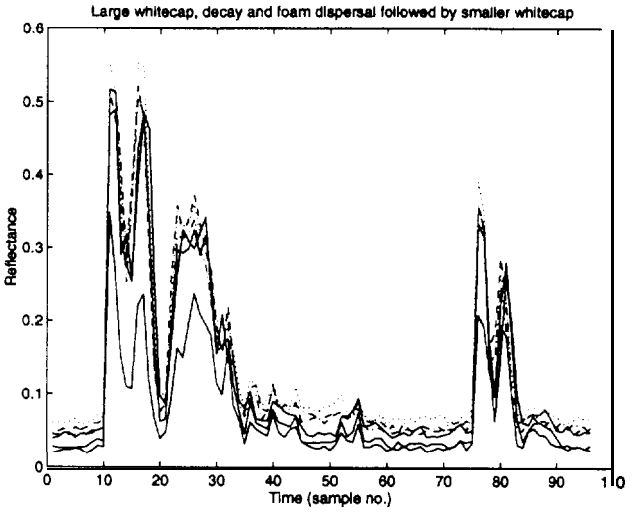

Figure 2-1. An ~ 15 second record of the reflectance of two whitecaps passing within the field of view of the radiometer. The lowest line corresponds to 860 nm.

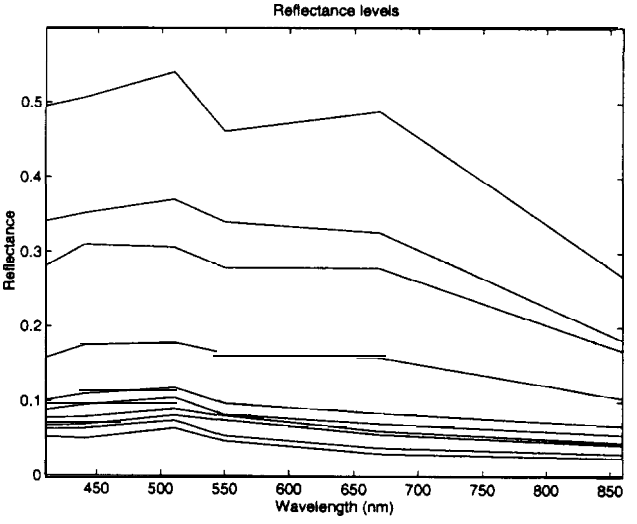

Figure 2–2. Spectral variation of the reflectance curves in Figure 2–1, sorted according to the magnitude of the spectrally averaged reflectance as described in the text.

whitecap of smaller magnitude (sample point 76) and continues to decay out to about sample point 96.

Figure 2-2 provides the spectral reflectance from these whitecaps for different levels of reflectance or foam types. The spectral shape of each level here is the mean of all reflectance values (averaged over wavelength) that fall within a reflectance interval. For this data, the lowest level corresponds to a reflectance between 0.04-0.05, followed by 0.05-0.06, 0.06-0.07, 0.07-0.08, 0.08-0.09, 0.09-0.1, 0.1-0.2, 0.2-0.3, 0.3-0.4 and highest level 0.4-0.5. The lower reflectance levels correspond to the non-whitewater reflectance. Of these, some are higher due to sky reflectance, others are lower due to shadowing by adjacent waves.

The variation in shape in each level is partly due to the small number of samples used in this graph. However, a common feature is the lower 670 and even lower 860 reflect ante values due the strong absorption by water at the longer wavelengths. A slight lower reflectance at the 410 channel is also observed.

Now, we examine a larger data set, acquired over 30 minutes, to provide a statistically better breakdown of the spectral reflectance of different foam types. In addition, we estimate the effective augmented reflectance contribution due to whitewater under the given wind and sea state condi-

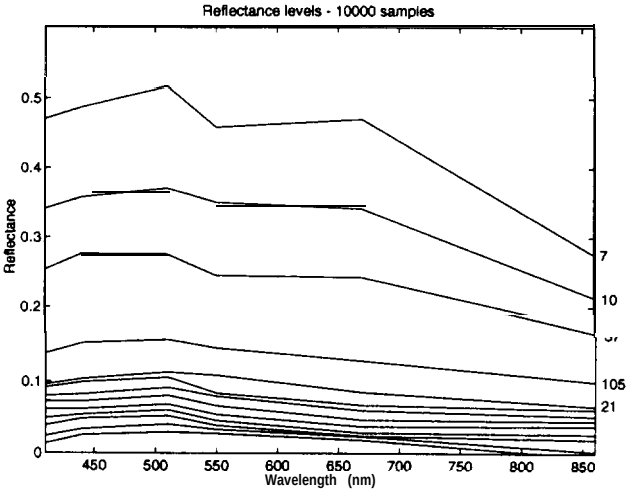

Figure 2–3. Same as Figure 2–2, but for a larger data set.

tions. In Figure 2–3, 10,000 samples are used. The number of occurrences of the top 5 reflectance levels is listed along the right-hand margin of the figure. This data set was acquired under overcast

condition, 11 AM, with wind speed ~ 12-13 m/s, air temperature 16.2° C and water temperature 17”C. The results are similar to those in Figure 2–2.

To estimate the augmented reflectance contribution from each reflectance level due to white-water, the frequency of occurrence of each reflectance level is multiplied by its spectral reflectance value and the background non whitewater reflectance subtracted. Determiningg the background non-whitewater reflectance is not always a simple matter. The background water reflectance can vary due to specular reflectance, sky reflectance (which in turn can be complicated by the sky condition, i.e., overcast, broken or clear), and by adjacent wave shadowing.

Using the same data set shown in Figure 2–3, examples of the estimated augmented reflectance contribution of whitewater are shown in Figure 2–4 for different estimates of the background water reflect ante, (a)- (d). In Panel (a), the augmented reflect ante contribution and the fractional coverage is known to contain a large portion of the background water reflectance and yields a high fraction coverage of 15.64%. Panel (b) shows the augmented reflect ante with what we believe to be all background water reflectance removed. This yields a fractional coverage of 4.07%. In Panel (c), more background is subtracted, so it is highly unlikely that this contains any background water reflectance; however, it may leave out some whitewater contribution. Its spectral shape is the result of both whitewater and foam. The spectral shape of the augmented reflectance in Panels (b) and (c) are almost identical. In Panel (d), too much background has been subtracted.

We believe that Figure 2-4b is the best estimate of the augmented reflectance, but it should be understood that a small variation in the determination of the background water reflectance could shift this estimate of fractional coverage to a slightly higher or lower value. The augmented reflectance contribution varies from a maximum of 0.0028 to a minimum of 0.0018 at 860 nm and is roughly ~ 35% of the value at 550 nm. This is consistent with the measurements of wave breaking in the surf zone, where *Frouin, Schwindling and Deschamps* [1996] determined the decrease in reflect ante at 860 nm to be 40%. The estimate of fractional coverage (4.0770) and augmented reflectance is also consistent with the fractional coverage found in the literature [Gordon ***and Wang, 1994],*** under fetch-limited conditions for wind speeds of 12-13 m/s.

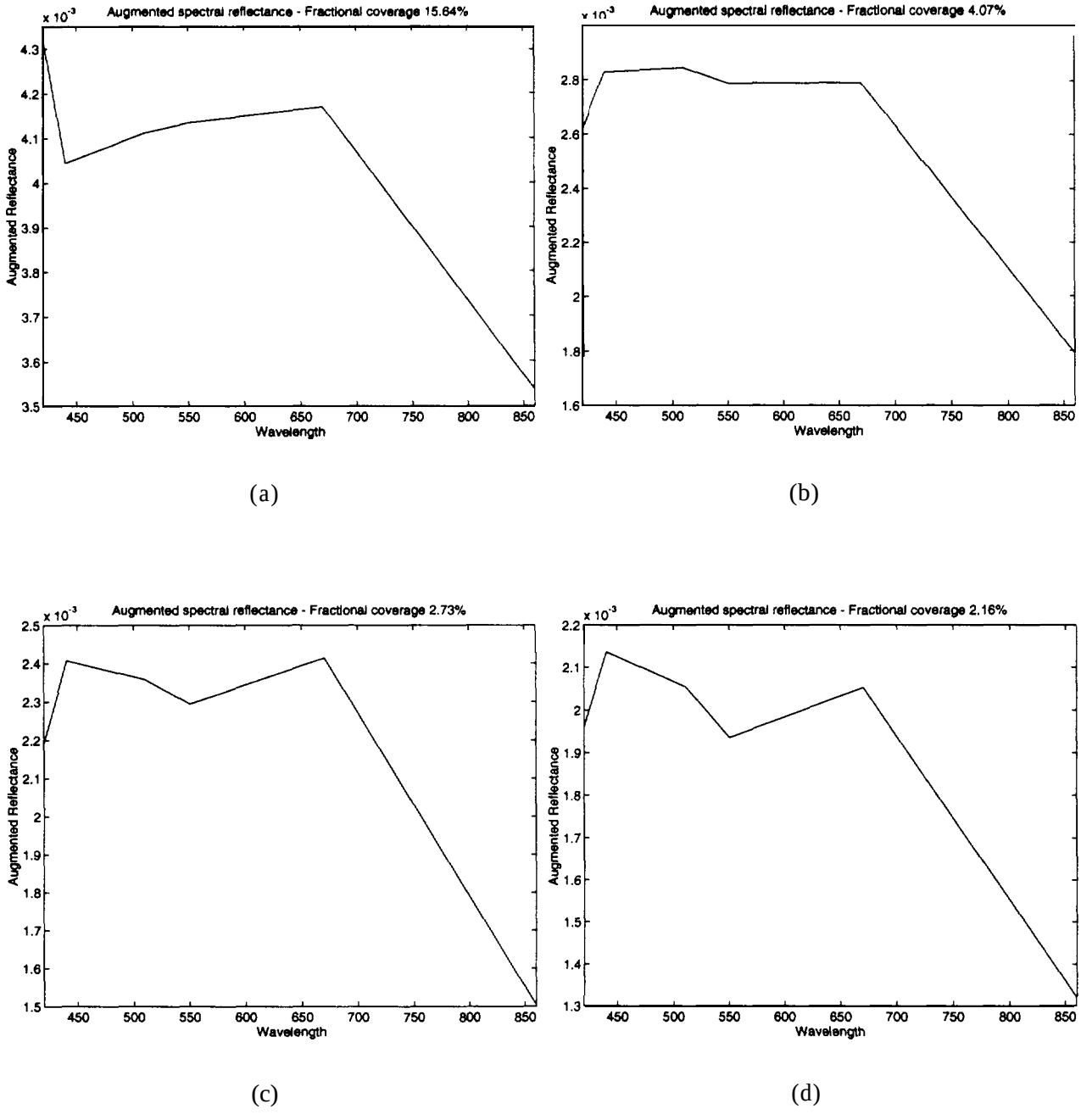

Figure 2-4. Augmented reflectance obtained by subtracting increasing amounts [(a) to (d)] of background water reflect ante. Panel (b) is believed to have the correct amount of background subtracted.

d. Anticipated Future Actions:

From preliminary results of the radiometric performance of the radiometer and deck cell under different sky conditions and solar angles, suggests the drop in reflectance at 860 nm may actually be

greater than that shown above. In addition, the drop in reflectance at 410 nm may also be explained and quantified as an artifact of the radiometer/deck cell performance. With this understanding, and with the more rigorous radiometric characterization that is now underway, the whitecap system will be deployed on another cruise. Another interesting aspect of whitecap reflectance that needs to be examined is the the effective change in whitecap reflectance at large solar zenith angles, where the protruding character of the whitecap above the ocean surface can efficiently reflect the red-rich light of the direct solar beam. This may warrant a cruise in high latitude waters where high zenith angles for much of the year are found over these colder waters, and where whitecaps may be of special importance to satellite observations.

e. Problems/Corrective Actions: None

f. Publications:

We are preparing two publications on this work. The fist is a description of the whitecap radiometer and the second describes the spectrum of the whitecap reflectance. An abstract “White-caps: Spectral reflectance in the open ocean and their contribution to water-leaving radiance,” by K.D. Moore, K.J. Voss, and H.R. Gordon, has been accepted for presentation at the SPIE Ocean Optics XIII Meeting.

3. In-water Radiance Distribution (with K. J. Voss).

a. Task Objectives:

The main objective in this task is to obtain upwelling radiance distribution data at sea for a variety of solar zenith angles to understand how the water-leaving radiance varies with viewing angle and sun angle.

b. Work accomplished:

Our efforts with the radiance distribution camera system were focused on the sky measurements during this period (See item 6 below),

c. Data/Analysis/Interpretation: none

d. Anticipated future actions:

We are looking for another opportunity to acquire data at sea. This will probably be on a cruise with Dennis Clark in the fall or winter.

e. Problems/Corrective actions: None.

f. Publications: None.

4. Residual Instrument Polarization.

a. Task Objectives:

The basic question here is: if the MODIS responds to the state of polarization state of the incident radiate, given the polarization-sensitivity characteristics of the sensor, how much will this degrade the performance of the algorithm for atmospheric correction?

b. Work Accomplished:

We have developed a formalism [*Gordon*, 1988] which provides the framework for removal of instrument al polarization-sensitivity effects. The difficulty with removing the polarization sensitivity y error is that the polarization properties of the radiance backscattered by the aerosol are unknown. Simulations of this effect for an instrument possessing ~ 3–4 times the polarization sensitivity expected for MODIS have been carried out. Analysis of the results suggest that elimination of the polarization effect is possible at the required level of accuracy by estimating the polarization of the top-of-atmosphere radiance to be that expected for a pure Rayleigh scattering atmosphere.

c. Data/ Analysis/Interpretation:

***See* b** above.

d. Anticipated Future Actions:

We will prepare a paper on the results of our simulations and correction scheme for publication. The goal will be submission dining of CY96

e. Problems/Corrective Actions: None

f. Publications: None,

5. Direct Sun Glint Correction.

a. Task Objectives: None.

6. Pre-launch Atmospheric Correction Validation (with K.J. Voss).

a. Task Objectives:

The long-term objectives of this task are four-fold:

(i) First, we need to study the aerosol phase function and its spectral variation in order to verify the applicability of the aerosol models used in the atmospheric correction algorithm. Effecting this requires obtaining long-term time series of the aerosol optical properties in typical maritime environments. This will be achieved using a CIMEL sun/sky radiometer that can be operated in a remote environment and send data back to the laboratory via a satellite link. These are similar the radiometers used by B. Holben in the AERONET Network. Thus, the objective is to acquire a CIMEL Automatic Sun Tracking Photometer, calibrate it, and deploy it in a suitable location for studying the optical properties of aerosols over the ocean.

(ii) Second, we must be able to measure the aerosol optical properties from a ship during the initialization/calibration/validation cruises. The CIMEL-type instrumentation cannot be used (due to the motion of the ship) for this purpose. The required instrumentation consists of an all-sky camera (which can measure the entire sky radiance, with the exception of the solar aureole region) from a moving ship, an aureole camera (specifically designed for ship use) and a hand-held sun photometer. We have a suitable sky camera and sun photometer and must construct an aureole camera. Our objective for this calendar year is (1) to assemble, characterize and calibrate the solar aureole camera system, (2) to develop data acquisition software, and (3) to test the system.

(iii) The third objective is to determine how accurately the radiance at the top of the atmosphere can be determined based on measurements of sky radiance and aerosol optical thickness at the sea surface. This requires a critical examination of the effect of radiative transfer on “vicarious” calibration exercises.

(iv) The forth objective is to utilize data from other sensors that have achieved orbit (MSX), or are expected to achieve orbit (OCTS, POLDER, SeaWiFS) prior to the launch of MODIS, to validate and fine-tune the correction algorithm.

b. Work Accomplished:

(i) During this last period we have constructed a filter changer assembly for the solar aureole camera system and performed numerous calibration and instrument performance checks. In addition we have improved the data acquisition system, allowing more rapid acquisition once the instrument is pointed at the sun.

The sky camera system has been modified and used to make measurements of the sky light polarization at several locations on several occasions. As we shall see in the discussion under (iii), this new polarization capability of the sky camera will be of considerable value in the initialization/calibration/validation work.

(ii) The CIMEL instrument was installed in the Dry Tortugas during this past quarter. The instrument we had purchased through this contract was found to have a problem and was sent back to CIMEL for repair. In the interim we borrowed an instrument from B. Holben (NASA/GSFC) and installed it at the site. This installation was successful and the instrument performed well in this marine environment. Recently we have replaced this instrument with our own instrument, and we have continued to have good results.

(iii) We have completed the survey phase of the examination of the effect of radiative transfer on "vicarious" calibration exercises and submitted a report to *Applied Optics*. This paper is now in press. Briefly, the radiance at the bottom of the atmosphere (BOA) and the aerosol optical thickness are inserted into a multiple-scattering inversion algorithm to retrieve the aerosol optical properties — the single scattering albedo and scattering phase function. These are then inserted into the radiative transfer equation to predict the radiance at the top of the atmosphere. Most of the simulations were carried out in the near infrared, where a larger fraction of the top of the atmosphere (TOA) radiance is contributed by aerosol scattering compared to molecular scattering, than in the visible, and where the water-leaving radiance can be neglected. The simulations suggest that the TOA radiate can be predicted with an uncertainty typically less than about 1% when the BOA radiances and the optical thickness measurements are error free. The influence of the simplifying

assumptions made in the inversion-prediction process, such as, modeling the atmosphere as a plane-parallel medium, employing a smooth sea surface in the inversion algorithm, using scalar radiative transfer theory, and assuming that the aerosol was confined to a thin layer just above the sea surface, was investigated. In most cases, these assumptions did not increase the error beyond l%. An exception was the use of scalar radiative transfer theory, for which the error grew to as much as ~ 2.5%. This suggests that using inversion and prediction codes that include polarization may be more appropriate. The uncertainty introduced by unknown aerosol vertical structure was also investigated and found to be negligible. Extension of the analysis to the blue, which requires the additional measurement oft he water-leaving radiance, showed significantly better predictions of the TOA radiance because the major portion of it is the result of molecular scattering, which is precisely known. We also simulated the influence of calibration errors in both the sun photometer and BOA radiometer. The results suggest that the relative error in the predicted TOA radiance is similar in magnitude to that in the BOA radiance (actually it is somewhat less). However, the relative error in the TOA radiance induced by error in optical thickness is usually << the relative error in optical thickness. Presently, it appears that radiometers can be calibrated with an uncertainty of ~ 2.5%, therefore it is reasonable to conclude that, at present, the most important error source in the prediction of TOA radiance from BOA radiance is likely to be error in the BOA radiate measurement.

(iv) We have been in contact with personnel involved with SeaWiFS, OCTS, and MSX to acquire data formats, and satellite data from these instruments to assess the validity of the atmospheric correction algorithm.

c. Data/ Analysis/Interpretation: None.

(i) We do not have real “at sea” data from the aureole camera to work with. We anticipate acquiring such data very early in this next quarter as discussed below.

(ii) The CIMEL instrument has been performing well in the Dry Tortugas. A sample long-term data record is shown in Figure 6–1. This data set will allow us to look at the variability of the optical signature of the marine aerosols, along with issues dealing with vicarious calibration of

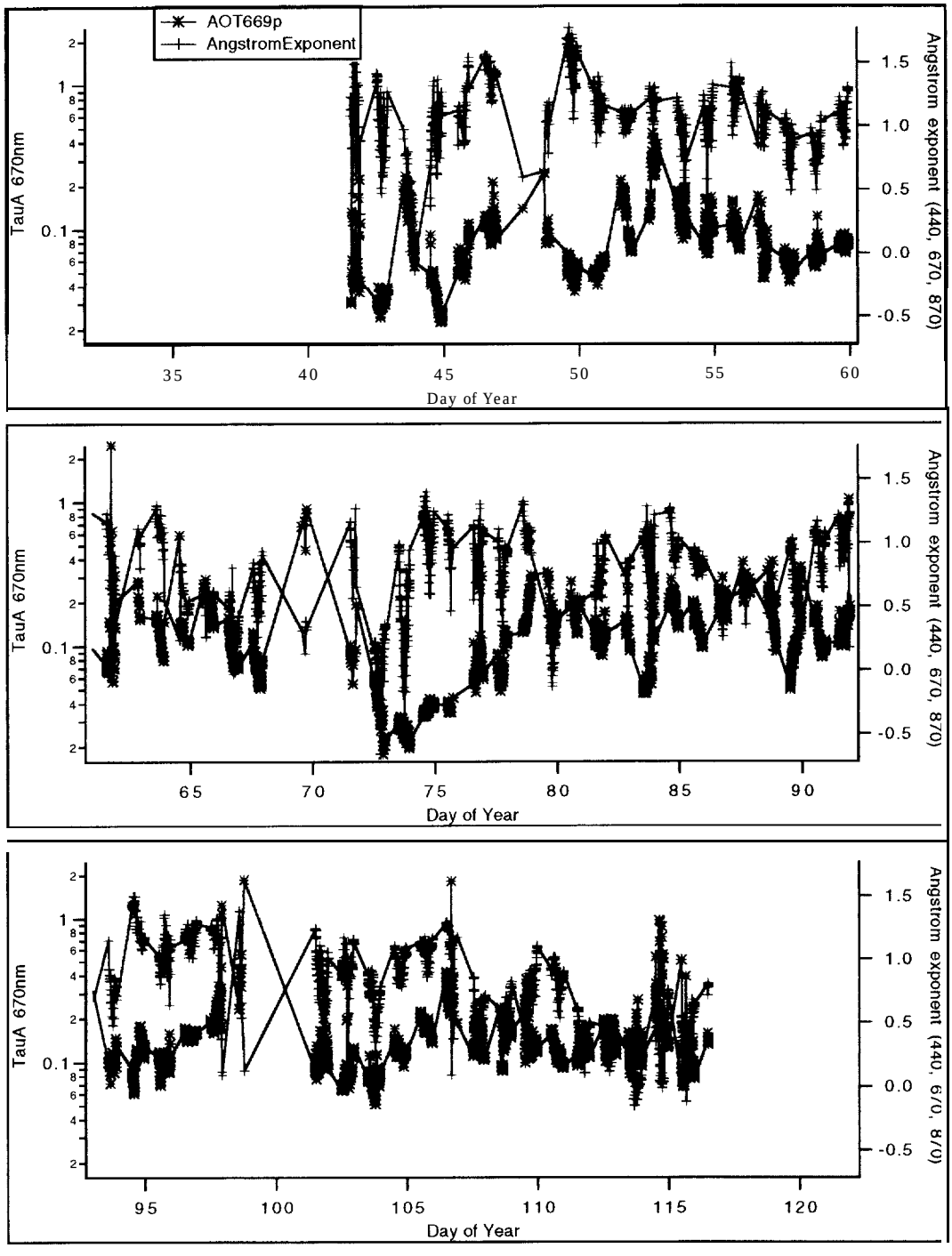

Figure 6-1. Time series of aerosol optical thickness (AOT) at 669 nm and Angstrom exponent at the Dry Tortugas test site.

the sensor. The figure shows the aerosol optical thickness (AOT) at 669 nm as a function of time at the site. Also shown is the Angstrom exponent ***n*** that describes the variation of the AOT with

wavelength λ according to AOT $(\lambda) \alpha \lambda^{-\eta}$. It noteworthy that the AOT is < 0.10 much of the time in winter, but proceeding into the spring it increases to 0.1–0.2 with a simultaneous decrease in ***n.*** These continuous measurements confirm the low values of AOT typically observed at sea *[Korotaev et al.,* 1993; *Reddy et al.,* 1990; *Villevalde et al.,* 1994].

Specific periods of time can also be investigated more closely as shown in Figure 6–2, which is an example of a 2-3 day period during which a cold front went through the measurement location. The missing data points are at night (no optical depth information is available at night). The cold front went through during the night of day 43 (43.0-43.5). After the cold front went through the

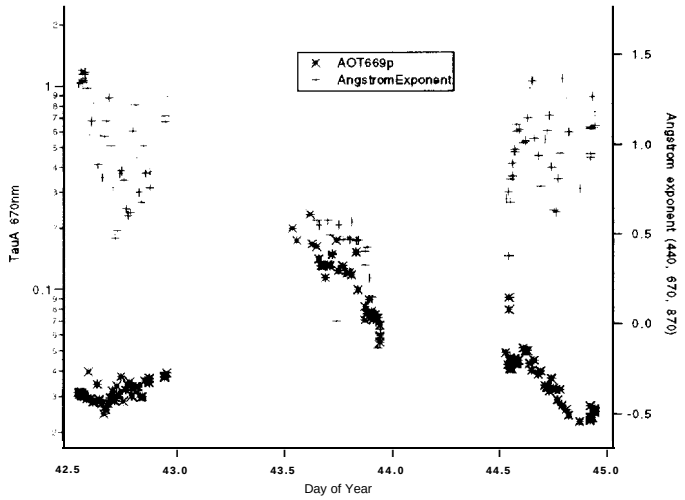

Figure 6–2. Spectral variation of τ, for the various stratospheric aerosol models. The cirrus cloud model is omitted because $\tau_s(\lambda)$is constant.

aerosol optical depth and Angstrom exponent decreased quite rapidly. The extreemly low values of the AOT after the passage of a cold front make this an ideal site for vicarious calibration in winter.

d. Anticipated Future Actions:

(i) We will be participating in the TARFOX experiment during July. TARFOX focuses on measuring atmospheric aerosols emanating from industrial centers in North America and transported over the Atlantic Ocean. Their extent, radiative properties, and transport mechanisms will

be studied from satellite, aircraft, and surface-based sensors. The monitoring effort will concentrate on the corridor extending from Wallops Island, Virginia to Bermuda. In situ aircraft, surface measurements, and satellite observations will simultaneously measure the chemical, physical, and optical properties of the predominant aerosols. This study provides a unique opportunity to validate current satellite remet e sensing methods, as well as to provide data needed for developing the atmospheric correction algorithm for regions subjected to absorbing urban aerosols. Brent Holben (NASA/GSFC) has arranged ship logistics to allow us to participate in TARFOX from a ship platform. This is required because the varied land albedo can affect the sky radiance and introduce unnecessary artifacts. The ship platform used is the cruise liner, Meridian. This ship will be making transects continually during the three weeks of TARFOX, between New York and Bermuda (the two of the sites of TARFOX are Wallops and Bermuda). This is an economical way to obtain sky measurements over the ocean, i.e., much cheaper than if a ship had been chartered specifically for this reason. We will be measuring the sky-radiance distribution, solar aureole, and direct solar irradiance during this field trip. instruments also on board operated by other personnel will be a CIMEL/ASSR, and a possibly a small LIDAR to provide vertical resolution.

In addition to this field trip we will be participating in field exercises with Dennis Clark in September and December in Hawaii. Once again during these trips we will be making field measurements of the sky radiance distribution, solar aureole, and solar irradiance along with some in- water measurements.

Finally, with the demonstration of the importance of the vertical structure in the presence of absorbing aerosols (Section 1 and Appendix 1), it is obvious that knowledge of the vertical structure of such aerosols is critical for developing a climatology to be used for their correction and for validation exercises. Thus, there is a clear need for ship-borne LIDAR to determine the vertical structure of the aerosol over the oceans, particularly in situations in which the aerosol is expected to be strongly absorbing, e.g., in the Saharan dust zone. Thus, during the remainder CY 96, we plan to procure a micropulse lidar (MPL) system for ship-borne use. Our goal is to acquire the system, learn its operation at Miami, and deploy in at sea, in December if possible.

(ii) We will continue to operate the CIMEL instrument in its location in the Dry Tortugas. The instrument is performing well and we do not anticipate problems other than routine maintenance. One issue we are working to resolve is receiving the data in a better format. We are now able to access the data over the network, but at times the speed of the internet line is not adequate. Work will be done in this quarter to address this problem.

(iii) We will develop a sky radiance inversion algorithm that utilized the full vector radiative transfer equation. This should remove the largest radiative transfer error in predicting the TOA radiance from the BOA radiance.

(iv) We will continue to try to obtain ocean color data from other sensors to assess the correction algorithm. We will procure a Unix work station dedicated to image processing that will be suitable for examination of such data and will provide the necessary image processing capability for the post-launch era.

e. Problems/corrective actions: None.

f. Publications:

H.R. Gordon and T. Zhang, How well can radiance reflected from the ocean-atmosphere system be predicted from measurements at the sea surface?, In press in ***Applied Optics.***

7. Detached Coccolith Algorithm and Post Launch Studies (W.M. Balch).

We participated in two cruises to the Gulf of Maine, a well known region for mesoscale coccolithophore blooms. We measured coccolithophore abundance, production and optical properties. A thorough understanding of the relationship between calcite abundance and light scatter, in coccolith-rich and coccolith-poor regions, will provide the basis for a generic suspended calcite algorithm.

a. Task Objectives:

The algorithm for retrieval of the detached coccolith concentration from the coccolithophorid, E. huxleyi is described in detail in our ATBD. The key is quantification of the backscattering coefficient of the detached coccoliths. Our earlier studies focussed on laboratory cultures to understand factors affecting the calcite-specific backscattering coefficient. As with algorithms for chlorophyll, and primary productivity, the natural variance between growth related parameters and optical properties needs to be understood before the accuracy of the algorithm can be determined. To this end, the objectives of our coccolith studies have been to define the effect of growth rate on:

(1) the rate that coccoliths detach from cells (this is also a function of turbulence and physical shear),

(2) rates of coccolith production

(3) morphology of coccoliths

(4) volume scattering and backscatter of coccoliths

For perspective on the directions of our work, we provide an overview of our previous activities. During 1995, we focussed on all of the above objectives using chemotstat cultures (in which algal growth rate is precisely controlled). During the latter half of 1995, our work focused on shipboard measurements of suspended calcite and estimates of optical backscattering as validation of the laboratory measurements. We participated on two month-long cruises to the Arabian sea, measuring coccolithophore abundance, production, and optical properties. During the first half of 1996, we

focused again on objectives 2 and 4, during two Gulf of Maine cruises, one in March and one in June.

b. Work Accomplished:

Our work during the last 6 months was mostly directed towards two cruises in the Gulf of Maine, a region known for its dense populations of coccolithophores. We have waited eagerly for an opportunity to take the flow-through instrument into the Gulf of Maine where the coccolithophore, Emiliania huxleyi forms large blooms. (Recall, that our previous cruises were to the Arabian Sea, a region not known for meso-scale coccolithophore blooms, but still containing moderately abundant coccolithophores.) We took our flow-through light scattering photometer, which uses a Wyatt Technologies laser-light scattering photometer equipped with a flow-through cell to measure volume scattering at 18 angles. Integration of this signal in the backward direction allows us to calculate backscattering in real time. During the first 6 months of 1996, we performed considerable programing and instrument interfacing in order to streamline the data flow. The system now monitors chlorophyll fluorescence, pH, temperate, salinity and 18-channel volume scatter. A Global Positioning System was interfaced, as well. The first cruise was in March, a very rough period in this region. We brought our flow-through light scattering detector which functioned flawlessly. In June, we ran 2000 miles of transects in the Gulf of Maine with our flow-through light scattering photometer and may have observed the early stages of coccolithophore bloom development in Wilkinson Basin. During both cruises, we also measured the rate of calcite production (from which we can calculate the turnover of calcite particles in the surface regions of the ocean).

c. **Data/Analysis/Interpretation:**

As expected, calcite-dependent backscattering was low in the Gulf of Maine during March, but it was still measurable. Typically, calcite scattering accounted for 5-10% of total backscattering. A very different picture was observed in June. Acid-labile scattering increased to 30-40% of total backscattering in Wilkinson Basin, a stratified basin in the middle of the Gulf of Maine. Acid-labile scattering dropped over Georges Bank as the predominant populations were diatoms, and values increased again in the Northeast Channel, similar to previous blooms that we have observed. The

observations are consistent with the calcite being produced in the more stable Wilkinson Basin with subsequent advection around the NE flank of Georges Bank. We are preparing for another Gulf of Maine cruise at the end of October, and again will be taking the flow-through system. Much of these data are still in the process of being worked-up.

Calcification measurements from the March 1996 cruise were remarkably high, given that this was at the beginning of the Spring bloom. We were finding >1070 of the carbon being fixed into coccoliths. This also explains the relatively high fraction of calcite-dependent light scattering seen during this time. Calcification rates are still being processed for the June cruise but preliminary results suggest that they were quite high.

d. Anticipated Future Actions:

We are currently performing data analysis for all previous cruise work and this work will continue into the next 6 months. The current state of the data are as follows:

(1) Suspended calcite samples are being run in the graphite furnace atomic absorption spectrometer at the University of Maine. We have completed about 1/5 of our sample backlog and expect the remainder to be done over the summeer.

(2) We have hired a full time technician to begin counting our 900 cell and coccolith counts. She is currently working on the Arabian Sea samples from 1995.

(3) All calcification data have been processed to units of gC $m^{-3} d^{-1}$ and integrated over the water column at each station. They still need to be processed into complete sections.

(4) Turnover of the calcite particles needs to be calculated for the Gulf of Maine cruises

(5) The underway data is now processed for temperature, salinity, pH, fluorescence and backscatter (with and without calcite) averaged over each kilometer of all trips. Following final calibration checks have been done for half of the underway data. Hydrographic plots will be made in which light scattering is plotted as a function of temperature and salinity.

(6) Of major interest in this data set will be the relationship between calcite-dependent backscattering (b'_b) and the concentration of suspended calcite or concentration of detached coccoliths. This will be of major relevance to our MODIS algorithm efforts. Besides actually checking our algorithm, the net result of these results will be to define the accuracy and precision of the algorithm, exceedingly import ant for subsequent interpretation.

We are continuing analysis of our previous flow cytometer results.

e. Problems/Corrective Actions: None

f. Publications:

Balch, W. M., K. A. Kilpatrick, P. M. Holligan and C. Trees. 1996. “The 1991 coccolithophore bloom in the central north Atlantic I. Optical properties and factors affecting their distribution.” In press. *Limnology and Oceanography.*

Balch, W. M., K. Kilpatrick, P. M. Holligan, D. Harbour, and E. Fernandez. 1996. “The 1991 coccolithophore bloom in the central north Atlantic II. Relating optics to coccolith concentration.)’ In press. *Limnology and Oceanography.*

Balch, W., M. and K. A. Kilpatrick. 1996. “Calcification rates in the equatorial Pacific along 140°W.” In press. *Deep Sea Research.*

8. Other Developments.

The PI participated in the MODIS Science Team review of MCST on January 23, 1996 at GSFC.

The PI participated in a conference call with MODIS Science Team members and MCST regarding the SBRS MODIS test schedule on March 8, 1996.

The PI, K.J. Voss, and W. M. Balch participated in the MODIS review meeting in Miami from 30 March to 5 April, 1996.

The PI collaborated with Dennis Clark and Ken Voss in a paper describing a detailed plan for validation of atmospheric correction of MODIS ocean bands. It was presented at the Workshop on Remote Sensing of Aerosols April 15-19 in Washington, D.C. This workshop was organized by Y. Kaufman, D. Tanre, T. Nakajima, and H. Gordon, and was supported by EOS.

The PI attended the MODIS Science Team meeting May, and prepared a memorandum for the MODIS Project Scientist regarding the use of the LIB MODIS data in tracking the MODIS radiometric calibration.

The PI attended the EOS Validation Workshop and chaired the “breakout” group on Validation of Atmospheric Correction of EOS Sensors. With F. Palluconi he prepared a summary report on the activities of the group.

In May we installed an AERONET CIMEL on Barbados at J. Prosperous aerosol monitoring site.

9. Publications, submissions, and abstracts for CY 96.

The following publications, submissions, and abstracts are attached to this report as appendices.

Appendix 1: H.R. Gordon, Atmospheric Correction of Ocean Color Imagery in the Earth Observing System Era, Revised to *Journal of Geophysical Research, Atmospheres.*

Appendix 2: H.R. Gordon, T. Zhang, F. He, and K. Ding, Effects of stratospheric aerosols and thin cirrus clouds on atmospheric correction of ocean color imagery: Simulations, Submitted to *Applied Optics.*

Appendix 3: H.R. Gordon and T. Zhang, How well can radiance reflected from the ocean-atmosphere system be predicted from measurements at the sea surface?, In press in *Applied Optics.*

Appendix 4: Balch, W. M., K. A. Kilpatrick, P. M. Holligan and C. Trees. 1996. "The 1991 coccolithophore bloom in the central north Atlantic I. Optical properties and factors affecting their distribution." In press in *Limnology and Oceanography.*

Appendix 5: Balch, W. M., K. Kilpatrick, P. M. Holligan, D. Harbour, and E. Fernandez. 1996. "The 1991 coccolithophore bloom in the central north Atlantic II. Relating optics to coccolith concentration." In press in *Limnology and Oceanography.*

Appendix 6: Balch, W., M. and K. A. Kilpatrick. 1996. "Calcification rates in the equatorial Pacific along 140° W." In press in *Deep Sea Research.*

Appendix 7: K.D. Moore, K.J. Voss, and H.R. Gordon, Abstract: "Whitecaps: Spectral reflectance in the open ocean and their contribution to water-leaving radiance," Accepted for presentation at the SPIE Ocean Optics XIII Meeting.

10. References.

Frouin, R., M. Schwindling and P. Y. Deschamps, Spectral reflectance of sea foam in the visible and near-infrared: In-situ measurements and implications for remet e sensing of ocean color and aerosols, *Jour. Geophys. Res., IOIC,* 14,361–14,371, 1996.

Gordon, H. R., Ocean Color Remote Sensing Systems: Radiometric Requirements, *Society of Photo-Optical Instrumentation Engineers, Recent Advances in Sensors, Radiometry, and Data Processing for Remote Sensing, 924,* 151-167, 1988.

Gordon, H. R., O. B. Brown, R. H. Evans, J. W. Brown, R. C. Smith, K. S. Baker and D. K. Clark, A Semi-Analytic Radiate Model of Ocean Color, *Jour. Geophys. Res., 93D,* 10909–10924, 1988.

Gordon, H. R. and M. Wang, Influence of Oceanic Whitecaps on Atmospheric Correction of Sea-WiFS, *Applied Optics, 33,* 7754-7763, 1994.

Korotaev, G. K., S. M. Sakerin, A. M. Ignatov, L. L. Stowe and E. P. McClain, Sun-Photometer Observations of Aerosol Optical Thickness over the North Atlantic from a Soviet Research Vessel for Validation of Satellite Measurements, *Jour. Atmos. Oceanic Technol., 10,* 725–735, 1993.

Morel, A. and B. Gentili, Diffuse reflectance of oceanic waters: its dependence on Sun angle as influenced by the molecular scattering contribution, *Applied Optics, 30,* 4427-4438, 1991.

Morel, A. and B. Gentili, Diffuse reflectance of oceanic waters. II. Bidirectional aspects, *Applied Optics, 32,* 6864-6879, 1993.

Reddy, P. J., F. W. Kreiner, J. J. Deluisi and Y. Kim, Aerosol Optical Depths Over the Atlantic Derived From Shipboard Sunphotometer Observations During the 1988 Global Change Expedition, *Global Biogeochemical Cycles, 4,* 225-240, 1990.

Shettle, E. P. and R. W. Fenn, Models for the Aerosols of the Lower Atmosphere and the Effects of Humidity Variations on Their Optical Properties, Air Force Geophysics Laboratory, Hanscomb AFB, MA 01731, AFGL-TR-79-0214, 1979.

Villevalde, Y. V., A. V. Smirnov, N. T. O'Neill, S. P. Smyshlyaev and V. V. Yakovlev, Measurement of Aerosol Optical Depth in the Pacific Ocean and North Atlantic, *Jour. Geophys. Res.*, *99D*, 20983-20988, 1994.

Appendix 7

WHITECAPS: SPECTRAL REFLECTANCE IN THE OPEN OCEAN AND THEIR CONTRIBUTION TO WATER LEAVING RADIANCE

Karl D. Moore, Ken J. Voss, Howard R. Gordon

Physics Dept., University of Miami
Coral Gables, FL 33124

Abstract: The reflectance of white water (foam) generated by whitecaps in the open ocean is obtained with a 6-channel spectral radiometer, extended from the bow of a ship, measuring the upwelling radiance from the water surface. Simultaneously, a 6-channel cosine collector measures the downwelling irradiance at the same wavelengths (410, 440, 510,550,670 and 860 rim). In addition to reflectance data, air / water temperature, wind speed and direction are obtained as well as GPS (global positioning system) information in order to characterize ocean surface conditions. A visual reference for sea surface conditions measured by the radiometer is recorded using a video camera mounted along side the radiometer. By measuring a small area of the water surface over time, the presence and spectral influence of whitecaps can be quantified. Using this technique the spectral reflectance of individual whitecaps can be measured and tracked through their complete life cycle. Also, integration over larger time series of ocean surface reflectance data provides a measurement of the augmented or extra contribution from white water reflectance to the water leaving radiance observed by ocean color satellites. Estimates of the augmented reflectance is subsequently correlated to sea surface state, and includes the frequency of occurrence and spectral contribution from various levels of white water reflectance as whitecaps grow and decay.

The effects of sky reflectance, sun glitter and specular reflectance are investigated in terms of setting the threshold between white water and non white water events and the consequences in accurately determining the augmented reflectance contribution. A brief discussion is provided of the impact of sky conditions (overcast/clear) during the measurement process and the implications of solar zenith angle on the water leaving radiance during whitecap conditions from nadir observing platforms.